Journal of Physics and Chemistry of Solids 128 (2019) 211–217

Contents lists available at ScienceDirect

Journal of Physics and Chemistry of Solids

journal homepage: www.elsevier.com/locate/jpcs

Pressure-induced superconductivity and quantum phase transitions in the Rashba material BiTeCl

M.L. Jin [a,b], S.J. Zhang [a,b,*], L.Y. Xing [a,b], W.M. Li [a,b], G.Q. Zhao [a,b], X.C. Wang [a,b], Y.W. Long [a,b], X.D. Li [d], H.Y. Bai [a,b], C.Z. Gu [a,b], C.Q. Jin [a,b,c,**]

[a] Institute of Physics, Chinese Academy of Sciences, Beijing 100190, China
[b] University of Chinese Academy of Sciences, Beijing 100049, China
[c] Collaborative Innovation Center of Quantum Matters, Beijing, China
[d] Institute of High Energy Physics, Chinese Academy of Sciences, Beijing, China

ARTICLE INFO

Keywords:
High pressure
Rashba semiconductor
Superconductivity

ABSTRACT

Recent theoretical predictions have indicated that BiTeX (X = Cl, Br, I) type strong spin orbital coupling semiconductor compounds with strong Rashba effects are suitable for use as topological insulators under compressed conditions and novel phenomena have been identified in experiments. The compound BiTeCl is expected to exhibit a topological nontrivial state under pressure. In this study, we obtained measurements based on the resistivity, Hall coefficient, synchrotron X-ray diffraction, and Raman spectroscopy using the Rashba semiconductor BiTeCl crystal at high pressures up to 54.8 GPa. Our experiments indicated that the Rashba semiconductor BiTeCl exhibited a pressure-induced metal to insulator-like transition at 2.8 GPa. A pressure-induced structural phase transition was observed above 5.5 GPa, which was followed by a superconducting transition. The superconducting transition temperature (T_C) increased to a maximum 4.2 K with pressures up to 32 GPa. Compared with BiTeI, the structural phase transition of BiTeCl occurs at a relatively lower pressure due to the weaker Rashba effects, where the inner chemical pressure is affected by the replacement of I with Cl.

1. Introduction

Strong spin orbital interactions play important roles in the formation of novel quantum states [1–3]. In the 1950s, Dresselhaus and Rashba determined the bulk spin orbit coupling (SOC) of odd parity in the electron's momentum p for non-centrosymmetric semiconductors [4,5]. The odd parity in p SOC with broken inversion symmetry is referred to as Rashba SOC and it has led to many discoveries and innovative concepts regarding the spin galvanic effect, spin Hall effect, topological insulators, Majorana fermion, Dirac materials, and cold atom systems [6].

The Rashba energy, E_R, and the momentum offset of split states, k_R, are two key operating characteristics for assessing the Rashba coupling strength as: $\boldsymbol{\alpha}_R = 2E_R/k_R$. In conventional Rashba semiconductors, the parameter $\boldsymbol{\alpha}_R$ is in the order of 10^{-1} eVÅ [7–9]. However, a much larger parameter $\boldsymbol{\alpha}_R$ is required for room-temperature applications of spintronics devices. The bismuth tellurohalides BiTeX (X = Cl, Br, I) possess bulk and surface states with large Rashba SOC, and they have attracted increasing attention recently. These three compounds share two similarities: a non-centrosymmetric layered structure with broken inversion symmetry; and quite similar electronic structures, where both the valence and conduction band states are characterized by splitting in terms of their energy and momentum. Materials containing one or more heavy elements are also expected to exhibit a topological phase transition, where the band inversion should be derived from the SOC interaction that underlies the Rashba effect. Recently, it was suggested that the Rashba effect can be used to produce a p-wave superconductor with very special edge-states such as Majorana bound states. High pressure is a powerful method for generating new quantum states in many topological materials [10–18]. A pressure-induced topological state and superconducting state have also been reported for BiTeI [19,20]. It is not clear whether topological superconductivity is induced in these materials. The order of the bulk gap value in BiTeX (X = Cl, Br, I) at ambient pressure is: BiTeCl > BiTeBr > BiTeI, whereas the order of the Rashba parameter value is the reverse (BiTeCl < BiTeBr < BiTeI) and it increases with the

* Corresponding author. Institute of Physics, Chinese Academy of Sciences, Beijing, China
** Corresponding author. Institute of Physics, Chinese Academy of Sciences, Beijing, China.
E-mail addresses: sjzhang@iphy.ac.cn (S.J. Zhang), Jin@iphy.ac.cn (C.Q. Jin).

https://doi.org/10.1016/j.jpcs.2017.09.024
Received 5 May 2017; Received in revised form 8 August 2017; Accepted 15 September 2017
Available online 21 September 2017

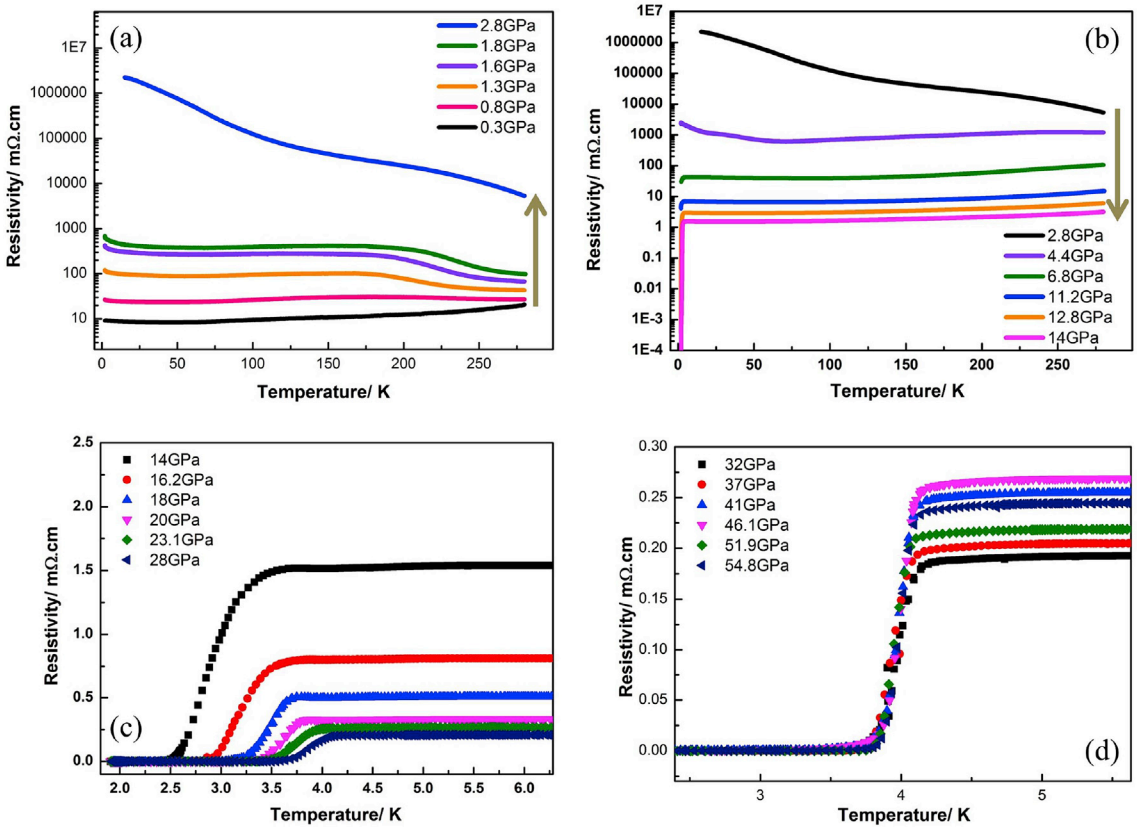

Fig. 1. (a, b) Resistivity of a single BiTeCl crystal as a function of temperature in the low pressure phase, showing the maximum resistivity at 2.8 GPa and the initial superconductivity transition at 6.8 GPa (c, d) Resistivity of a single BiTeCl crystal as a function of temperature in the high-pressure range from 14 to 54.8 GPa.

atomic number of the halogen elements [21].

In this study, we determined the superconductivity induced in BiTeCl by pressure at the transition from a Rashba type semiconductor to an insulating state. The ambient phase of BiTeCl crystallizes into a non-centrosymmetric layered structure with a hexagonal space group $P6_3mc$ [22]. Thus, we investigated its structural evolution including local structure distortion at high pressure by using Raman spectroscopy and high pressure synchrotron X-ray diffraction (XRD).

2. Methods

Single crystals of BiTeCl were grown using the Bridgeman method. The Te powder, Bi, and Cl reagents were mixed together at an appropriate stoichiometric ratio, before the mixture was ground thoroughly in an agate mortar to ensure homogeneity. The mixture was sealed in an evacuated quartz tube under 10^{-4} Pa and heated to 660 °C for 24 h, followed by slow cooling at a rate of 12°C/h to 100 °C before quenching to room temperature [20].

The electronic transport properties of BiTeCl were measured using four-probe electrical conductivity methods in a diamond anvil cell (DAC) made of CuBe alloy. The diamond culet had a diameter of 300 μm. Au wires with a diameter of 18 μm were used as electrodes. The T301 stainless steel gasket was compressed from a thickness of 250 to 40 μm, and then drilled with a hole measuring 150 μm in diameter. Cubic BN used as an insulating layer was pressed into this hole and a small hole was drilled in the center with a diameter of 100 μm as a sample chamber, where NaCl fine powder was loaded as a pressure transmitting medium and a single BiTeCl crystal with dimensions of 60 μm × 60 μm × 15 μm. A piece of ruby was also loaded as a pressure marker. The DAC was placed inside a Maglab system with automatic temperature control. A thermometer was mounted near the diamond to monitor the temperature. The high pressure Hall coefficients were measured using the Van der Paul method.

High-pressure Raman experiments were conducted using a single crystal BiTeCl with dimensions of 70 μm × 70 μm × 20 μm in a DAC using a Renishaw inVia Raman microscope at a laser wavelength of 532 nm and spectral resolution of ~1 cm^{-1}. Silicon oil was used as the pressure medium. The diamond culet measured 300 μm in diameter. The T301 stainless steel gasket was compressed from 250 μm to 40 μm and a hole measuring 140 μm in diameter was drilled in the center. A tiny ruby was placed beside the specimen to measure the pressure.

High pressure synchrotron XRD experiments were performed at the Institute of High Energy Physics, Chinese Academy of Sciences, at a wavelength of 0.6199 Å in a symmetric DAC with a culet that measured 300 μm in diameter. The T301 steel gasket was pre-indented from 250 μm to ~40 μm and a hole was drilled in the center with a diameter of 150 μm. The sample was placed in the hole with silicon oil as a near hydrostatic pressure transmitting medium. Ruby balls were placed near the sample as pressure markers. The XRD patterns were acquired with a MAR 3450 image plate detector. The two-dimensional image plate patterns were converted into one-dimensional 2θ versus the intensity data using the Fit2D software package [23].

3. Results and discussion

3.1. High pressure electrical transport properties of a single BiTeCl crystal

Fig. 1 shows the changes in the resistivity of a single BiTeCl crystal as a function of temperature up to 54.8 GPa, which indicates that the resistivity exhibited metallic behavior below 0.8 GPa, as reported previously [20,24]. The lower resistivity at ambient pressure is usually attributed to the carriers due to defects. We observed that the resistivity increased dramatically by six orders of magnitude at low temperature from ambient pressure to 2.8 GPa, as shown in Fig. 1a, thereby indicating

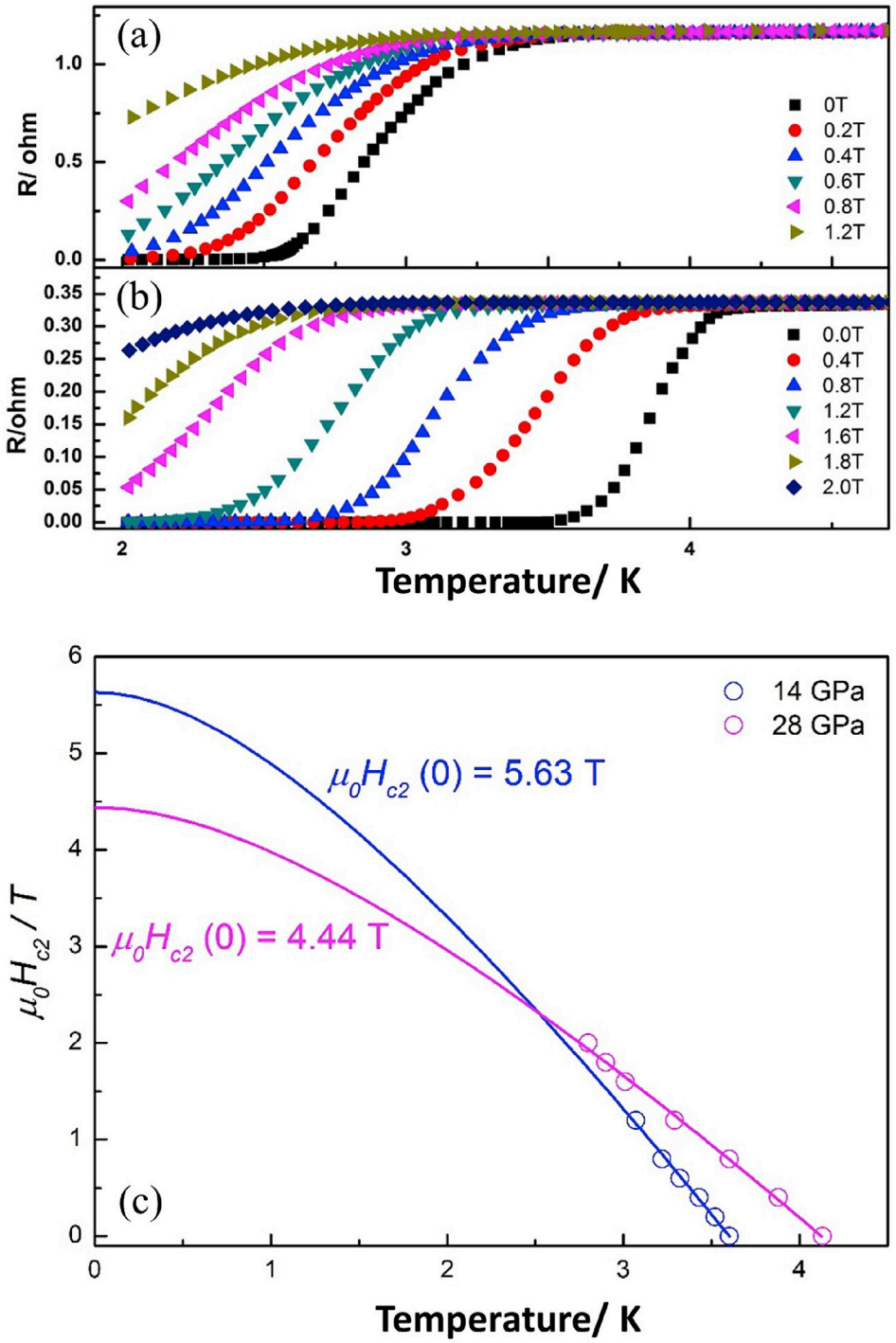

Fig. 2. (a, b) Magnetic field dependence of the superconductivity transition by a single BiTeCl crystal at 14 GPa and 28 GPa with an applied magnetic field *H* perpendicular to the *a*–*b* plane. (c) The magnetic field versus T_C^{onset}. The blue circle and magenta circle denote the experimental data obtained at 14 GPa and 28 GPa, respectively. The solid lines indicate fits to the data based on the Werthdamer–Helfand–Hohenberg theory. (For interpretation of the references to colour in this figure legend, the reader is referred to the web version of this article.)

a phase transition from a Rashba type semiconductor to an insulating state. As the pressure increased further, the resistivity gradually decreased and superconductivity appeared at 6.8 GPa when metallic behavior was exhibited (Fig. 1b). However, we noted that the first appearance of superconductivity occurred in a normal insulating state in our previous study [25]. This difference may be explained mainly by the different defects in the BiTeCl samples used in the two studies. T_C increased up to 32 GPa and then remained stable up to 54.8 GPa, as shown in Fig. 1c and d.

The superconductivity was validated based on resistance measurements obtained under a variable external magnetic field, as shown in Fig. 2. Fig. 2a and b show that T_C decreased as the magnetic field *H* applied perpendicular to the a–b plane of the BiTeCl single crystal increased at 14 GPa and 28 GPa, which demonstrates that the transition was to superconductivity. The magnetic field versus T_C^{onset} is shown in Fig. 2c. The upper critical field $\mu_0 H_{c2}(0)$ values at 14 GPa and 28 GPa were 5.63 T and 4.44 T, respectively, which we estimated using the Werthdamer–Helfand–Hohenberg formula [26].

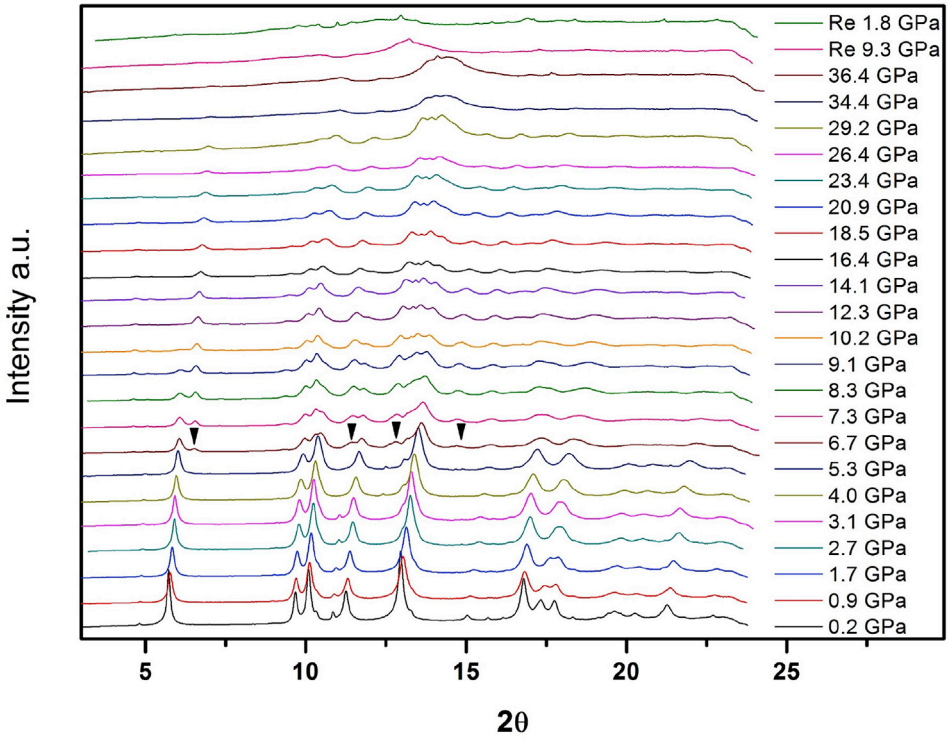

Fig. 3. X-ray diffraction patterns obtained for BiTeCl up to 36.4 GPa.

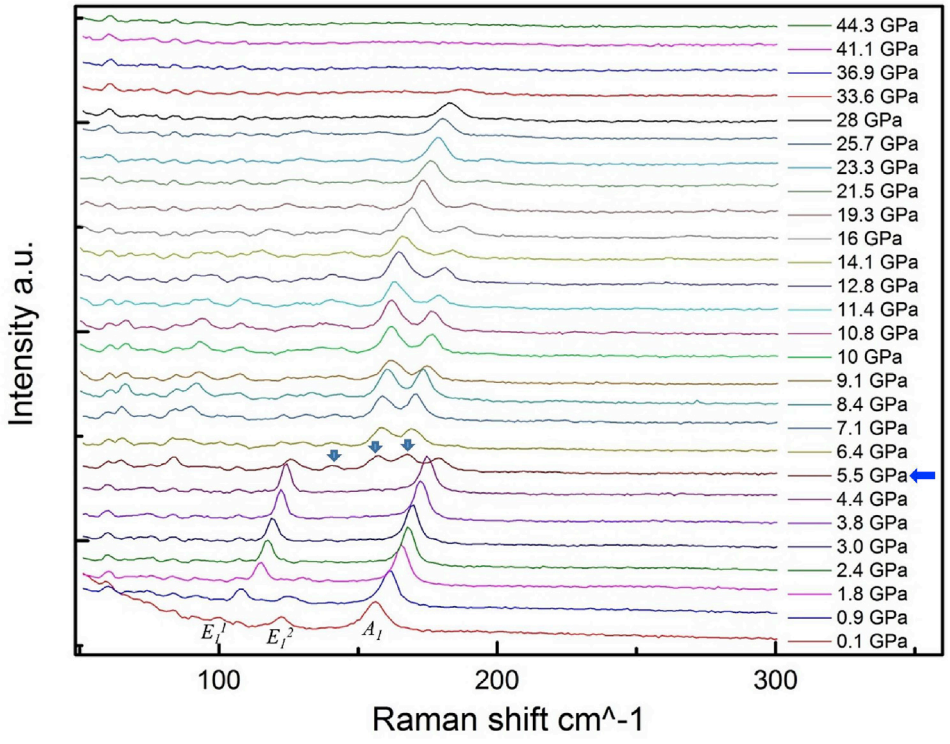

Fig. 4. Raman spectra obtained for BiTeCl as a function of pressure.

3.2. *High pressure structural transitions in a BiTeCl crystal*

High pressure angle dispersive XRD (ADXRD) measurements of BiTeCl were obtained to determine the source of the different quantum state transitions with respect to the changes in the crystal's structure (Fig. 3). The ambient phase of BiTeCl crystallizes into a non-centrosymmetric layered structure with a hexagonal $P6_3mc$ space group. The first pressure-induced structural transition was observed above 6.7 GPa and the second structural transition was observed above 34.4 GPa, as shown in Fig. 3.

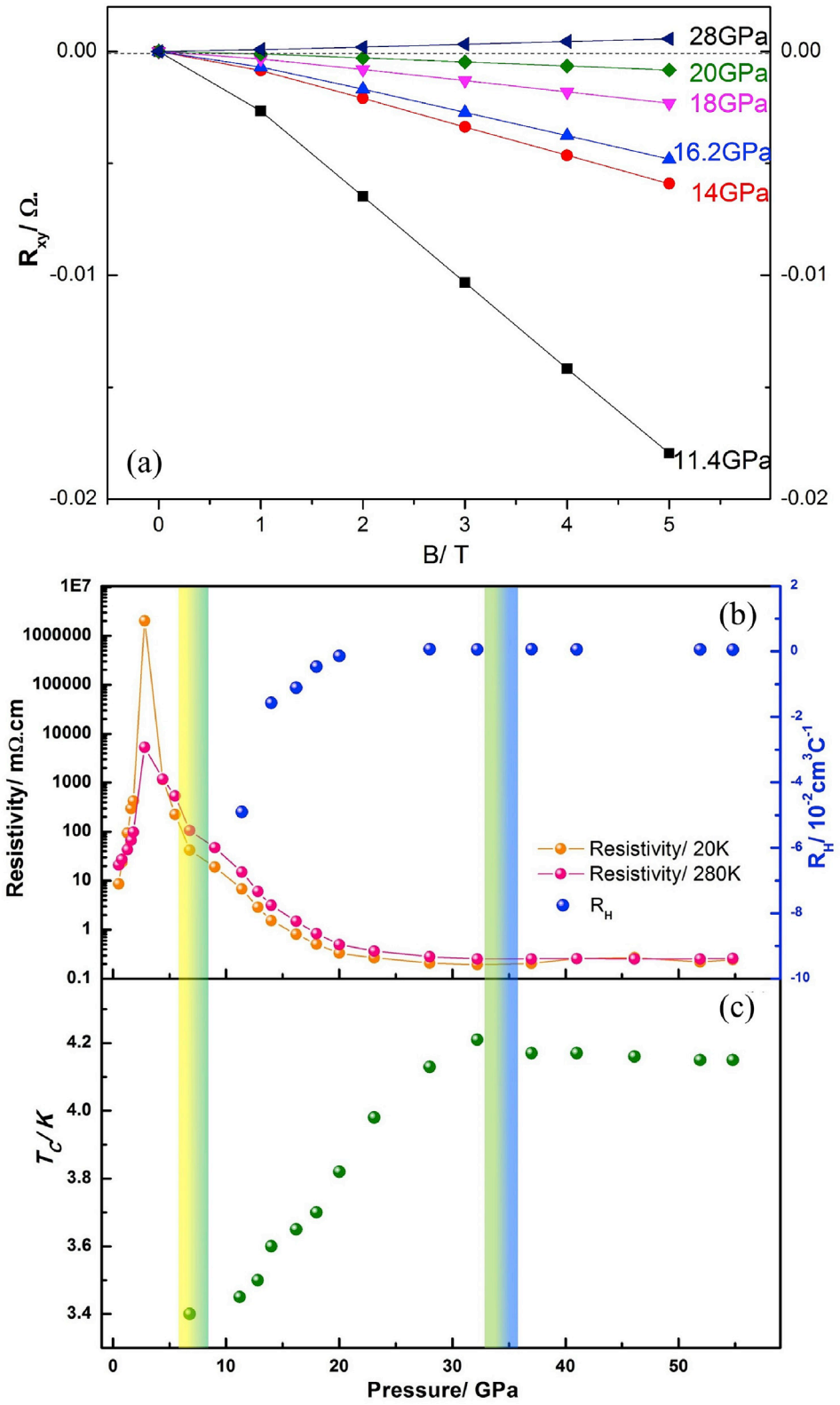

Fig. 5. (a) Hall resistance obtained for BiTeCl as a function of the applied pressure, which shows the approximately linear behavior with a transition from a negative slope to a positive slope. (b) Resistivity obtained for a single BiTeCl crystal at temperatures of 20 K and 280 K up to 54.8 GPa, and with the Hall coefficient R_H fixed at 20 K as a function of pressure. The transition from a Rashba semiconductor state to an insulator-like state is indicated by the maximum resistivity P_C ~2.8 GPa. The Hall coefficient R_H changed from negative to positive above 28 GPa. (c) Superconducting transition temperature (T_c) as a function of pressure. The first superconducting transition appeared at ~6.8 GPa with T_C onset at 3.4 K, followed by extension into the region up to 54.8 GPa.

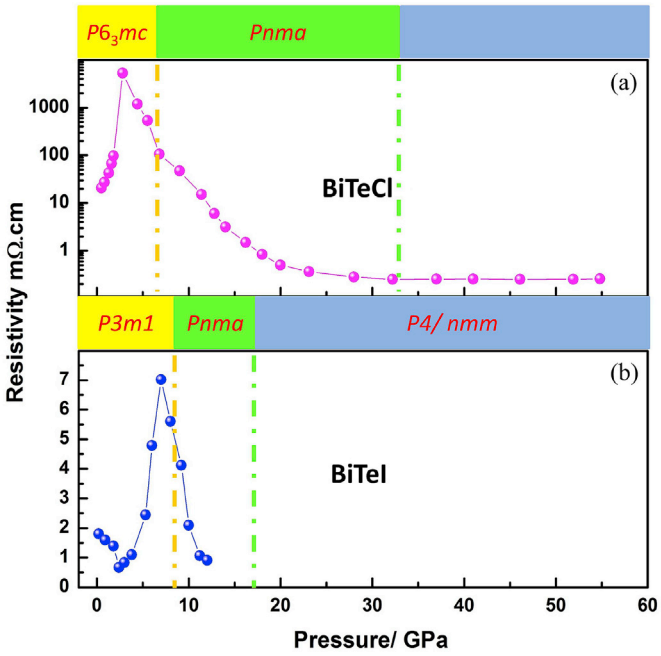

Fig. 6. Resistivity obtained for (a) BiTeCl and (b) BiTeI at 280 K as a function of pressure.

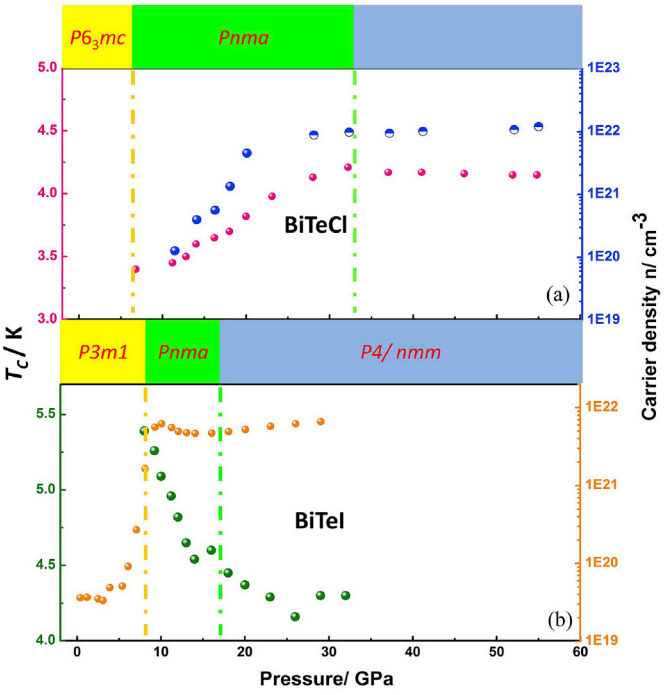

Fig. 7. Superconducting transition temperature (T_c) and carrier density at 20 K for (a) BiTeCl and (b) BiTeI as a function of pressure.

Raman spectroscopy was performed to obtain insights into the local structural changes at high pressure, as shown in Fig. 4. Raman spectroscopy is sensitive to local bond vibrations and symmetry breaking, so it provided evidence of the changes in the properties of BiTeCl under high pressure. The ambient pressure phase of BiTeCl has seven Raman active modes ($2A_1 + 2E_1 + 3E_2$). Sklyadneva et al. [27] stated that both of the *E*-type (E_1 in BiTeCl) modes involve in-plane vibrations of the Bi, Te, and Cl layers, where the lower *E* mode has a larger contribution from the vibration of the Cl atom. The highest observed mode was A_1 symmetry [27], which is produced by the motion of the Bi and Te sublattices against each other along the polar axis. This A_1 mode is independent of the halogen atom, so it is at approximately the same frequency in BiTeBr and BiTeI, i.e., around 152 cm^{-1} [20,28]. We observed three primary phonon modes in BiTeCl, with the lower E_1^1 mode at 99.7 cm^{-1}, the higher E_1^2 mode at 122.4 cm^{-1}, and the A_1 mode at 156.2 cm^{-1}. All three modes shifted to high frequencies below 5.5 GPa, while the E_1^2 mode softened and disappeared at 2.4 GPa. Interestingly, a metal-like to insulator-like transition occurred at 2.8 GPa, which is close to the pressure where E_1^2 disappeared. This softening may have contributed to the superconductivity promoted by strong electron–phonon coupling. Above 5.5 GPa, the emergence of new modes and the disappearance of the A_1 and E_1^1 modes in the Raman spectra indicated a transition to a high pressure phase. Above 33.6 GPa, no Raman modes were detected in the measurement range (<300 cm^{-1}) for BiTeCl, which may be attributed to the second phase transition, as observed by ADXRD above 34.4 GPa. Previous XRD measurements and calculations for BiTeI indicated an orthorhombic *Pnma* structure above 8.9 GPa and a tetragonal *P4/nmm* structure above 16 GPa [20]. Similarly, an orthorhombic *Pnma* structure above 6.7 GPa was determined for BiTeBr [28]. The *Pnma* phase is considered to occur for BiTeX (X = Cl, Br, I) compounds at high pressures because most V-VI-VII semiconductors crystallize into this structure [29,30]. According to the high pressure ADXRD analysis of BiTeCl, as shown in Fig. 3, we considered a phase transition from the hexagonal *P6$_3$mc* structure to an orthorhombic *Pnma* structure above 5.5 GPa, and a second phase transition to a higher symmetric structure with a possible cubic unit cell.

The Hall resistance analysis of BiTeCl versus the magnetic field at 20 K as a function of the applied pressure is shown in Fig. 5a. The Hall resistance exhibited approximately linear behavior as a function of a strong magnetic field. The slope had a negative value that increased with the applied pressure and it changed to a positive slope above 28 GPa, thereby indicating that the carrier changed from electron dominant to hole dominant under pressure. The resistivity at 20 K and 280 K, the Hall coefficient R_H at 20 K, and T_C as functions of pressure are shown in Fig. 5b and c. The transition from a Rashba semiconductor state to an insulating state occurred in the ambient phase, as indicated by the maximum of resistivity at P_C ~2.8 GPa. The first superconducting transition appeared at ~6.8 GPa with T_C onset of 3.4 K, where the structure transformed from the *P6$_3$mc* phase into the *Pnma* phase. T_C increased from 3.4 to 4.1 K below 28 GPa, where the pressure range of R_H also increased with the pressure. T_C and R_H remained stable at higher pressures up to 54.8 GPa.

Figs. 6 and 7 compare the single BiTeCl and BiTeI crystals in terms of their resistivity at 280 K, carrier density at 20 K, and T_C as functions of pressures. For BiTeI with the ambient phase of *P3m1*, the topological phase transition resulted in a V-shaped change in the resistivity at P_C ~2 GPa [20]. By contrast, for BiTeCl with the ambient phase of *P6$_3$mc*, the transition from a Rashba semiconductor with a metal-like behavior to an insulator-like state yielded a Λ-shaped change in the resistivity at P_C ~2.8 GPa, with much higher resistivity than BiTeI. A previous structural study [31] indicated that a semi-ionic model with a polar axis along the atomic stacking direction can be employed to describe the structure of BiTeX (X = Cl, Br, I), with a corrugated $(BiTe)^+$ layer and X^- anions in the ambient phase. The larger resistivity of BiTeCl may be explained by the stronger electron binding force induced by the smaller unit cell and the smaller ionic size of Cl^- compared with that of I^-. The first structural phase transition pressure for BiTeCl (>5.5 GPa) was lower than that for BiTeI (>7.5 GPa). The smaller unit cell and ionic size could introduce additional inner chemical pressure in BiTeCl, as well as contributing to the weaker Rashba SOC due to the conventional expectation that heavy elements have reasonably high atomic SOC. Theoretically, it has also been demonstrated that the Rashba parameter [21] is smaller for BiTeCl than that for BiTeI, while that for BiTeBr is intermediate, and the order of the structural transition pressures [32] is the same as that stated above (BiTeCl < BiTeBr < BiTeI), where it increases with the atomic number of the halogen elements. We found that in the BiTeX system, compounds

with weaker Rashba effects exhibited structural transitions at lower pressures. The second structural phase transition pressure was much higher for BiTeCl (34.4 GPa) than that for BiTeI (16 GPa). Above the first structural transition pressure, the resistivity of both compounds decreased with pressure to the 10^{-1} mΩ × cm level. Similarly, superconductivity appeared in both compounds after the structural phase transitions, as shown in Fig. 7. For BiTeCl, T_C increased to a maximum as the carrier density increased below 28 GPa, where both the T_C and carrier density remained stable after the carrier types transformed from n dominant to p dominant. By contrast, for BiTeI, the superconductivity appeared when the carrier density increased to a maximum, and T_C then decreased as the carrier density remained stable. BiTeI is considered to be a superconductor near the Rashba-type topological transition where it is transformed from a Rashba-type semiconductor. Similar to BiTeI, the superconductivity of BiTeCl appears close to the insulator-like phase where it is also transformed from a Rashba-type semiconductor.

4. Conclusions

In this study, we performed resistivity, Hall coefficient, synchrotron XRD, and Raman spectroscopy analyses of a BiTeCl crystal as a Rashba material at high pressures up to 54.8 GPa. We successfully observed pressure-induced transitions by this spin orbital interaction compound from a Rashba-type semiconductor to an insulator-like state, followed by a classical quantum condensation (i.e., superconductivity). We systematically compared the properties of BiTeCl and BiTeI. In the BiTeX system, compounds with weaker Rashba effects exhibit structural transitions at lower pressures and superconductivity appears after the structural phase transition.

Acknowledgments

This work was supported by the National Key Research and Development Program of China (2016YFA0300300), and the National Basic Research Program of China (2015CB921000).

References

[1] A.P. Mackenzie, Y. Maeno, The superconductivity of Sr_2RuO_4 and the physics of spin-triplet pairing, Rev. Mod. Phys. 75 (2003) 657.
[2] G. Cao, T.F. Qi, L. Li, J. Terzic, S.J. Yuan, L.E. DeLong, G. Murthy, R.K. Kaul, Novel magnetism of $Ir^{5+}(5d^4)$ ions in the double perovskite Sr_2YIrO_6, Phys. Rev. Lett. 112 (2014), 056402.
[3] L. Fu, C.L. Kane, Superconducting proximity effect and Majorana fermions at the surface of a topological insulator, Phys. Rev. Lett. 100 (2008), 096407.
[4] G. Dresselhaus, Spin-orbit coupling effects in zinc blende structures, Phys. Rev. 100 (1955) 580.
[5] E.I. Rashba, Properties of semiconductors with an extremum loop. 1. Cyclotron and combinational resonance in a magnetic field perpendicular to the plane of the loop, Sov. Phys. Solid State 2 (1960) 1109–1122.
[6] A. Manchon, H.C. Koo, J. Nitta, S.M. Frolov, R.A. Duine, New perspectives for Rashba spin-orbit coupling, Nat. Mater. 14 (2015) 871–882.
[7] J. Nitta, T. Akazaki, H. Takayanagi, T. Enoki, Gate control of spin-orbit interaction in an inverted $In_{0.53}Ga_{0.47}As/In_{0.52}Al_{0.48}As$ heterostructure, Phys. Rev. Lett. 78 (1997) 1335.
[8] G. Lommer, F. Malcher, U. Rossler, Spin splitting in semiconductor heterostructures for B→ 0, Phys. Rev. Lett. 60 (1988) 728–731.
[9] J. Luo, H. Munekata, F.F. Fang, P.J. Stiles, Effects of inversion asymmetry on electron energy band structures in GaSb/InAs/GaSb quantum wells, Phys. Rev. B 41 (1990) 7685.
[10] J.L. Zhang, S.J. Zhang, H.M. Weng, W. Zhang, L.X. Yang, Q.Q. Liu, S.M. Feng, X.C. Wang, R.C. Yu, L.Z. Cao, L. Wang, W.G. Yang, H.Z. Liu, W.Y. Zhao, S.C. Zhang, X. Dai, Z. Fang, C.Q. Jin, Pressure-induced superconductivity in topological parent compound Bi_2Te_3, Proc. Natl. Acad. Sci. 108 (2011) 24–28.
[11] S.J. Zhang, J.L. Zhang, X.H. Yu, J. Zhu, P.P. Kong, S.M. Feng, Q.Q. Liu, L.X. Yang, X.C. Wang, L.Z. Cao, W.G. Yang, L. Wang, H.K. Mao, Y.S. Zhao, H.Z. Liu, X. Dai, Z. Fang, S.C. Zhang, C.Q. Jin, The comprehensive phase evolution for Bi_2Te_3 topological compound as function of pressure, J. Appl. Phys. 111 (2012), 112630.
[12] J.L. Zhang, S.J. Zhang, H.M. Weng, W. Zhang, L.X. Yang, Q.Q. Liu, P.P. Kong, J. Zhu, S.M. Feng, X.C. Wang, R.C. Yu, L.Z. Cao, S.C. Zhang, X. Dai, Z. Fang, C.Q. Jin, Superconductivity of topological matters induced via pressure, Front. Phys. 7 (2012) 193–199.
[13] J. Zhu, J.L. Zhang, P.P. Kong, S.J. Zhang, X.H. Yu, J.L. Zhu, Q.Q. Liu, X. Li, R.C. Yu, R. Ahuja, W.G. Yang, G.Y. Shen, H.K. Mao, H.M. Weng, X. Dai, Z. Fang, Y.S. Zhao, C.Q. Jin, Superconductivity in topological insulator Sb_2Te_3 induced by pressure, Sci. Rep. 3 (2013) 2016.
[14] P.P. Kong, J.L. Zhang, S.J. Zhang, J. Zhu, Q.Q. Liu, R.C. Yu, Z. Fang, C.Q. Jin, W.G. Yang, X.H. Yu, J.L. Zhu, Y.S. Zhao, Superconductivity of the topological insulator Bi_2Se_3 at high pressure, J. Phys. Condens. Matter 25 (2013) 362204.
[15] P.P. Kong, F. Sun, L.Y. Xing, J. Zhu, S.J. Zhang, W.M. Li, Q.Q. Liu, X.C. Wang, S.M. Feng, X.H. Yu, J.L. Zhu, R.C. Yu, W.G. Yang, G.Y. Shen, Y.S. Zhao, R. Ahuja, H.K. Mao, C.Q. Jin, Superconductivity in strong spin orbital coupling compound Sb_2Se_3, Sci. Rep. 4 (2014) 6679.
[16] L.P. He, Y.T. Jia, S.J. Zhang, X.C. Hong, C.Q. Jin, S.Y. Li, Pressure-induced superconductivity in the three-dimensional topological Dirac semimetal Cd_3As_2, NPJ Quant. Mater. 1 (2016) 16014.
[17] Y. Liu, Y.J. Long, L.X. Zhao, S.M. Nie, S.J. Zhang, Y.X. Weng, M.L. Jin, W.M. Li, Q.Q. Liu, Y.W. Long, R.C. Yu, C.Z. Gu, F. Sun, W.G. Yang, H.K. Mao, X.L. Feng, Q. Li, W.T. Zheng, H.M. Weng, X. Dai, Z. Fang, G.F. Chen, C.Q. Jin, Superconductivity in $HfTe_5$ across weak to strong topological insulator transition induced via pressures, Sci. Rep. 7 (2017), 44367.
[18] J. Zhu, A.R. Oganov, W.X. Feng, Y.G. Yao, S.J. Zhang, X.H. Yu, J.L. Zhu, R.C. Yu, C.Q. Jin, X. Dai, Z. Fang, Y.S. Zhao, Pressure induced Ag_2Te polymorphs in conjunction with topological non trivial to metal transition, AIP Adv. 6 (2016), 085003.
[19] M.S. Bahramy, B.J. Yang, R. Arita, N. Nagaosa, Emergence of non-centrosymmetric topological insulating phase in BiTeI under pressure, Nat. Commun. 3679 (2012) 679.
[20] M.L. Jin, F. Sun, L.Y. Xing, S.J. Zhang, S.M. Feng, P.P. Kong, W.M. Li, X.C. Wang, J.L. Zhu, Y.W. Long, H.Y. Bai, C.Z. Gu, R.C. Yu, W.G. Yang, G.Y. Shen, Y.S. Zhao, H.K. Mao, C.Q. Jin, Superconductivity bordering Rashba type topological transition, Sci. Rep. 7 (2017), 39699.
[21] L. Moreschini, G. Autès, A. Crepaldi, S. Moser, J.C. Johannsen, K.S. Kim, H. Berger, Ph Bugnon, A. Magrez, J. Denlinger, E. Rotenberg, A. Bostwick, O.V. Yazyev, M. Grioni, Bulk and surface band structure of the new family of semiconductors BiTeX (X= I, Br, Cl), J. Electron Spectrosc. Rel. Phenom. 201 (2015) 115–120.
[22] A. Akrap, J. Teyssier, A. Magrez, P. Bugnon, H. Berger, A.B. Kuzmenko, D. Van Der Marel, Optical properties of BiTeBr and BiTeCl, Phys. Rev. B 90 (2014), 035201.
[23] A.P. Hammersley, S.O. Svensson, M. Hanfland, A.N. Fitch, D. Hausermann, Two-dimensional detector software: from real detector to idealised image or two-theta scan, High. Pres. Res. 14 (1996) 235–248.
[24] J.A. Sans, F.J. Manjón, A.L.J. Pereira, R. Vilaplana, O. Gomis, A. Segura, A. Muñoz, P. Rodríguez-Hernández, C. Popescu, C. Drasar, P. Ruleova, Structural, vibrational, and electrical study of compressed BiTeBr, Phys. Rev. B 93 (2016), 024110.
[25] J.J. Ying, V.V. Struzhkin, Z.Y. Cao, A.F. Goncharov, H.K. Mao, F. Chen, X.H. Chen, A.G. Gavriliuk, X.J. Chen, Realization of insulating state and superconductivity in the Rashba semiconductor BiTeCl, Phys. Rev. B 93 (2016), 100504.
[26] N.R. Werthamer, E. Helfand, P.C. Hohenberg, Temperature and purity dependence of the superconducting critical field, Hc2. III. Electron spin and spin-orbit effects, Phy. Rev. 147 (1966) 295.
[27] I. Yu Sklyadneva, R. Heid, K.-P. Bohnen, V. Chis, V.A. Volodin, K.A. Kokh, O.E. Tereshchenko, P.M. Echenique, E.V. Chulkov, Lattice dynamics of bismuth tellurohalides, Phys. Rev. B 86 (2012), 094302.
[28] Unpublished results.
[29] E. Dönges, Über Chalkogenohalogenide des dreiwertigen Antimons und Wismuts. I. Über Thiohalogenide des dreiwertigen Antimons und Wismuts, Z. Anorg. Allg. Chem. 263 (1950) 112–132.
[30] A. Kikuchi, Y. Oka, E. Sawaguchi, Crystal structure determination of SbSI, J. Phys. Soc. Jpn. 23 (1967) 337–354.
[31] A.V. Shevelkov, E.V. Dikarev, R.V. Shpanchenko, B.A. Popovkin, Crystal structures of bismuth tellurohalides BiTeX (X = Cl, Br, I) from X-ray powder diffraction data, J. Solid State Chem. 114 (1995) 379–384.
[32] I.P. Rusinov, T.V. Menshchikova, I. Yu Sklyadneva, R. Heid, K.-P. Bohnen, E.V. Chulkov, Pressure effects on crystal and electronic structure of bismuth tellurohalides, New J. Phys. 18 (2016), 113003.